PHOTONICS Research

Spectrally flat supercontinuum generation in a holmium-doped ZBLAN fiber with record power ratio beyond 3 μm

Linyong Yang,[1] Bin Zhang,[1,2,3] Ke Yin,[1] Tianyi Wu,[1] Yijun Zhao,[1,2,3] and Jing Hou[1,2,3,*]

[1]College of Advanced Interdisciplinary Studies, National University of Defense Technology, Changsha 410073, China
[2]Hunan Provincial Key Laboratory of High Energy Laser Technology, Changsha 410073, China
[3]Hunan Provincial Collaborative Innovation Center of High Power Fiber Laser, Changsha 410073, China
*Corresponding author: houjing25@sina.com

Received 24 January 2018; revised 26 February 2018; accepted 26 February 2018; posted 28 February 2018 (Doc. ID 320378); published 18 April 2018

A spectrally flat mid-infrared supercontinuum (MIR-SC) spanning 2.8–3.9 μm with a maximum output power of 411 mW was generated in a holmium-doped ZBLAN fiber amplifier (HDZFA). A broadband fiber-based SC covering the 2.4–3.2 μm region was designed to seed the amplifier. Benefiting from the broadband seed laser, the obtained SC had a high spectral flatness of 3 dB over the range of 2.93–3.70 μm (770 nm). A spectral integral showed that the SC power beyond 3 μm was 372 mW, i.e., a power ratio of 90.6% of the total power. This paper, to the best of our knowledge, not only demonstrates the first spectrally flat MIR-SC directly generated in fluoride fiber amplifiers, but also reports the highest power ratio beyond 3 μm obtained in rare-earth-doped fluoride fiber until now.

OCIS codes: (320.6629) Supercontinuum generation; (140.3510) Lasers, fiber; (060.4370) Nonlinear optics, fibers; (060.2320) Fiber optics amplifiers and oscillators.

https://doi.org/10.1364/PRJ.6.000417

1. INTRODUCTION

Broadband mid-infrared supercontinuum (MIR-SC) laser sources have been a research focus due to their promising applications and great demand in a wide range of fields including biomedicine [1], environmental sensing [2], homeland security [3], and infrared spectroscopy [4]. Unfortunately, silica fibers, i.e., the most mature fibers cannot be used to obtain MIR-SC (typically >3 μm) due to a high phonon energy [5]. In fact, the long wavelength edge (LWE) of silica-fiber-based SC was limited to ~2.7 μm [6]. As a substitute, soft-glass fibers such as fluoride (ZBLAN and InF_3) [7,8], telluride [9], and chalcogenide [10] glass fibers with lower loss in MIR region have been developed. Among these alternatives, fluoride fibers are the best candidate for 3–5 μm SC generation if loss spectrum and maturity of manufacturing technique are both taken into consideration [11]. Besides, fluoride fibers are also used as transition fibers for SC spectrum extension into the deeper MIR region in chalcogenide fibers [12], where a high power ratio of long-wavelength region (typically beyond 3 μm) is preferred. Nevertheless, most passive fluoride fiber-based SCs have a large portion of residual shortwave components resulting from the typical 1.55 μm or 2 μm waveband pump sources [13–15]. Consequently, promoting long-wavelength power ratio is of significance, and the most straightforward scheme is to generate MIR-SC directly in rare-earth-doped soft-glass fibers.

An in-amplifier SC generation scheme has been a trend in recent few years where high output power and excellent compactness are insured [6,16]. Recently Gauthier *et al.* demonstrated MIR-SC generation in a heavily erbium-doped fluorozirconate (Er^{3+}:ZrF_4) fiber amplifier using the $^4I_{11/2} \rightarrow {}^4I_{13/2}$ transition [17]. Such an amplifier was seeded by a 2.75-μm optical parametric generation (OPG) with a pulse repetition rate (PRR) of 2 kHz and a pulse duration of 400 ps. A MIR-SC with a maximum output power of 154 mW and a spectral range of 2.6–4.1 μm was obtained. The authors claimed that power ratio beyond 3 μm was up to 82%, which was much higher than that of typical passive-ZBLAN-fiber-based SC [13]. Of course, the system in Ref. [17] was not specially designed for spectrally flat SC output.

Among the in-amplifier SC generation schemes, thulium-doped fiber amplifiers (TDFAs) seeded by broadband ultrafast pulses with a spectral range of 1.5–2 μm have performed high-spectral-flatness short-wave infrared SCs benefiting from cascaded mechanisms of amplification and Raman soliton self-frequency-shift (SSFS) [6,18]. In such reports, the broadband ultrafast seed pulses were obtained in passive silica fibers

pumped by 1550-nm laser pulses basically on nanosecond scale. Furthermore, in the MIR region, in-amplifier spectrally flat SC generation is also desirable but could be achieved only if a broadband seed laser with suitable wavelength (covering the gain band of holmium or erbium ions at 3-μm waveband) was obtained. Very recently, germania fibers have been proven rather useful to obtain broadband SC lasers up to 3 μm [19,20], which perfectly cover the 3-μm gain band of Er^{3+} and Ho^{3+} [11].

In this paper, a cascaded amplification and frequency-shift configuration was proposed for spectrally flat MIR-SC generation, which includes three stages of amplification process (via Er^{3+}, Tm^{3+}, and Ho^{3+}, respectively) and frequency-shift process (via passive fibers). In such a configuration, a holmium-doped ZBLAN fiber amplifier (HDZFA) served as the main amplifier, which was seeded by a broadband pulsed laser based on germania-core fiber (GCF). The obtained SC had a broadband spectrum spanning from 2.8 to 3.9 μm with a maximum output power of 411 mW. Up to 90.6% of the output power was located above 3 μm. In the meanwhile, high spectral flatness with a 3-dB range of 2.93–3.70 μm was ensured. This is the first report of spectrally flat in-amplifier MIR-SC generation seeded by a broadband fiber laser.

2. EXPERIMENTAL SETUP AND RESULTS

Figure 1 depicts the schematic of the spectrally flat MIR-SC source. The whole SC source comprises of a broadband seed laser spanning the 2.4–3.2 μm region and an HDZFA. The broadband seed laser had a similar structure as we had reported recently [20], which was comprised of a 1550-nm pulsed laser, an erbium–ytterbium-codoped fiber amplifier (EYDFA), a piece of single-mode fiber (SMF1), a single-mode thulium-doped fiber amplifier (TDFA), a mode field adapter (MFA), and a piece of GCF. The HDZFA consists of a piece of 4.5-m-long HDZF pumped by a homemade continuous wave (CW) 1150-nm ytterbium-doped fiber laser. The parameters of used fibers are listed in Table 1. The 1550-nm pulsed laser was an electrically modulated distributed feedback (DFB) laser with a tunable PRR and pulse duration of 40–100 kHz and

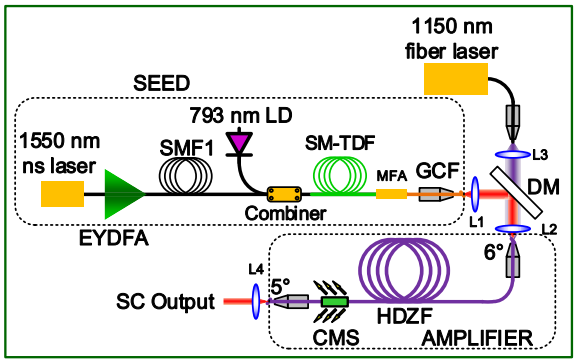

Fig. 1. Experimental setup of spectrally flat MIR-SC source. EYDFA, erbium–ytterbium-doped fiber amplifier; SMF, single-mode fiber; LD, laser diode; SM-TDF, single-mode thulium-doped fiber; MFA, mode field adapter; GCF, germania-core fiber; DM, dichroic mirror; HDZF, holmium-doped ZBLAN fiber; CMS, cladding-mode stripper; SC, supercontinuum.

Table 1. Specifications for the Used Fibers

Fiber Type	Core/Clad Diam. (μm)	Core/Clad NA (-)
EYDF	10/125	0.12/0.46
SMF1	8/125	0.14/-
SM-TDF	10/130	0.15/0.46
MFA (SMF2)	7/125	0.20/-
GCF	8/125	0.65/-
HDZF	10/125	0.16/0.46

1.6–10 ns, respectively. First, the 1550-nm seed pulses were power-scaled in the EYDFA. Then, the pulses were broken into numerous ultrafast pulses with higher peak intensity induced by nonlinearity of modulation instability (MI) [13], and red-shifted towards the 2-μm region in SMF1 under the mechanism of soliton dynamics (e.g., soliton fission and Raman SSFS). Afterwards, the 2-μm waveband soliton pulses were power-scaled in the TDFA and thereafter extended their spectrum towards 2.7 μm. The output fiber of the MFA was a SM fiber (SMF2). Next, in the following short piece of GCF, the 2.0–2.7 μm solitons were further redshifted, and the obtained spectrum covered a broad range of ~1.9–3.2 μm with a maximum power of ~300 mW. Such spectrum was a combination of numerous broadband soliton pulses [6]. A spectral integral showed that 32 mW of the total power (10.6%) was located in the 2.9–3.0 μm region, which overlapped the gain band of the used HDZF in this research. Finally, the broadband SC laser was coupled into a piece of HDZF via an aspheric lens (L1, 1–3-μm anti-reflection coated), a dichroic mirror (DM, with 95% reflectivity among 2.4–3.2 μm and 95% transmissivity at 1.15 μm), and a CaF_2 lens (L2), with a total coupling efficiency of ~14%. The 1150-nm light, i.e., the pump light of the HDZFA, was coupled into the HDZF via two CaF_2 lenses (L2, L3) with a launching efficiency of 70%. Both ends of the HZDF were angle-cleaved (at 6° and 5°, respectively) in order to avoid back-reflected light coupled into the core of HDZF. The residual pump power was evacuated by a cladding mode stripper (CMS in Fig. 1) made of high-index polymer ($n = 1.64$). The generated SC light was collimated by another CaF_2 lens (L4) before spectral measurement. The used HDZF has a dopant concentration of 2 mol. % and a cladding absorption coefficient of ~1 dB/m. Since the calculated zero dispersion wavelength of this HDZF was ~1.62 μm, the signal of the 2.9–3.0 μm region is well located in the anomalous dispersion regime. Therefore, the dominant mechanisms in HDZFA are similar to those in TDFA reported in Ref. [6]. The SC-characterizing system includes a grating-based monochromator together with a liquid-nitrogen-cooled InSb detector to measure the spectrum, and a wavelength-insensitive thermopile power meter to measure the output power.

Figure 2 shows the spectra measured at different positions. As could be seen, three stages of amplification and frequency-shift process were cascaded to form the cascaded amplification and frequency-shift configuration: erbium, thulium, and holmium gain bands were exploited for power amplification one by one; correspondingly, silica, germania, and ZBLAN fibers were used for spectral broadening under mechanism of soliton dynamics (mainly by soliton fission and Raman SSFS [15]).

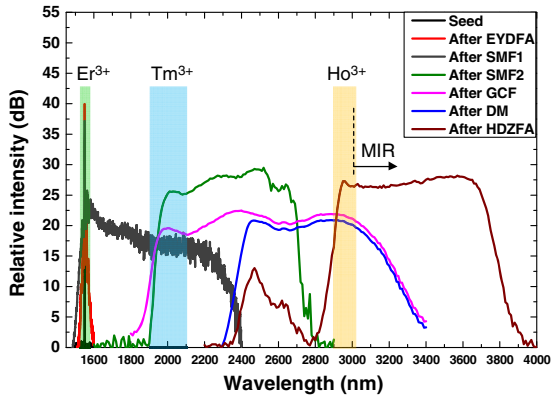

Fig. 2. Spectra comparison for different positions.

In the experiment, the evolution of SC spectra against launched pump power with repetition rate of 40 kHz was investigated first. The measured spectra were plotted in Fig. 3(a). As could be seen, though the broadband seed laser coupled into HDZF had a spectral range of 2.4–3.2 μm, the spectral component that could be effectively amplified was located at 2.9–3.0 μm. The spectral dip among 2.6–2.85 μm was mainly accounted for by the absorption of the $^5I_7 \rightarrow {}^5I_6$ transition (inverse process of desired $^5I_6 \rightarrow {}^5I_7$ transition). As pump power was increased, at first amplification of 2.9–3.0 μm was observed, after which spectral broadening appeared. As mentioned before, the dominant nonlinear mechanism in the process of spectral broadening was soliton fission and Raman SSFS due to the anomalous dispersion regime [6]. The LWE of the SC spectra continually extended towards longer wavelength until it reached 3.9 μm under the maximum available launched pump power of 5.9 W. At this time, the LWE seemed to be limited, and further spectral extension was almost stopped. The main cause that hinders further spectral broadening towards >4 μm was believed to be excited-state absorption (ESA) of the $^5I_6 \rightarrow {}^5I_5$ transition. In fact, Schneide *et al.* reported a holmium-doped fluoride fiber laser operating at 3.9 μm using the $^5I_5 \rightarrow {}^5I_6$ transition [21]. Besides, the LWE of the obtained SC in this experiment was apparently not halted by ZBLAN material loss. Therefore, it is highly reasonable that the ESA of the $^5I_6 \rightarrow {}^5I_5$ transition was the main cause of the limited spectral bandwidth of the SC.

Then, SC spectra under different PRRs (40, 50, and 100 kHz) with same pulse duration of 1.6 ns were investigated. SC spectra with different PRRs of 40, 50, and 100 kHz at pump power of 5.91 W were plotted in Fig. 3(b). The spectra under 50 and 40 kHz were essentially identical and the SC's LWE reached 3.9 μm, which was longer than that under a repetition rate of 100 kHz (3.8 μm). Under the circumstance of 100 kHz, the power spectral density was obviously higher than that of 40 or 50 kHz in the range of 2.9–3.5 μm, but the SC spectrum has a shorter LWE, which was mainly due to the reduced pulse peak power brought on by the doubled repetition rate. Under maximum pump power, the power ratio among 2.4–2.8 μm shown in Fig. 3 was calculated to be a negligible value of 0.58%, 0.61%, and 0.54% for 40, 50, and 100 kHz by spectral integral, respectively. Owing to the scheme of broadband soliton amplification, high spectral flatness was obtained. Under the condition of 50 kHz, the 3-dB spectral coverage was 2.93–3.70 μm.

To investigate the slope efficiency of HDZFA as a function of PRR, the output power was measured and shown in Fig. 4, under PRR of 100, 50, and 40 kHz, respectively. For these situations, the slope efficiency with respect to launched (absorbed) pump power was located among 6.3% (9.8%) to 7.5% (11.6%). Increasing the PRR (or, increasing pulse duty ratio) from 40 to 100 kHz did not bring significant enhancement to the slope efficiency. The weak signal and the low signal coupling efficiency were mainly responsible for the low slope efficiency of the HDZFA. Under circumstances of 50 kHz and 40 kHz, a slight decrease in slope efficiency was observed under the launched pump power over 4 W, which was mainly accounted for by the above-mentioned ESA of Ho^{3+} when the SC's LWE reached the absorption band of the $^5I_6 \rightarrow {}^5I_5$ transition. Even so, the best performance in the present research was obtained under 50 kHz, 1.6 ns, where a maximum output power of 411 mW with a broadest spectrum at 2.8–3.9 μm was

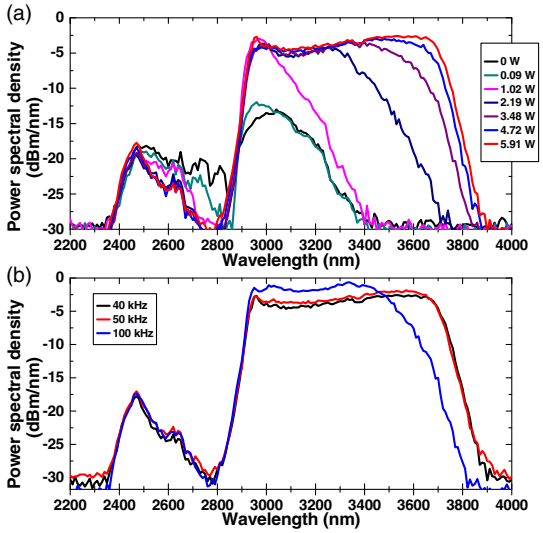

Fig. 3. (a) Evolution of SC spectra against launched pump power at 40 kHz; (b) SC spectra comparison under different PRRs at pump power of 5.91 W.

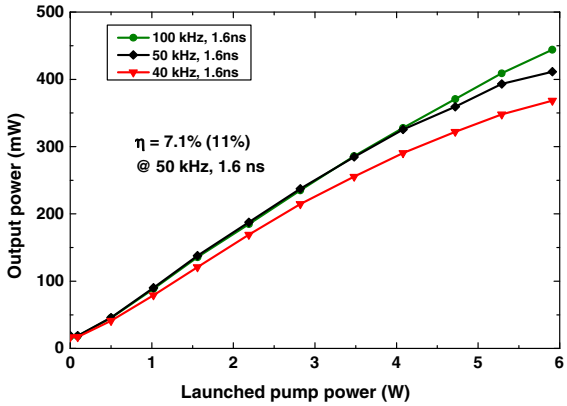

Fig. 4. SC average output power as a function of the launched pump power under different pulse repetition rates with pulse duration of 1.6 ns.

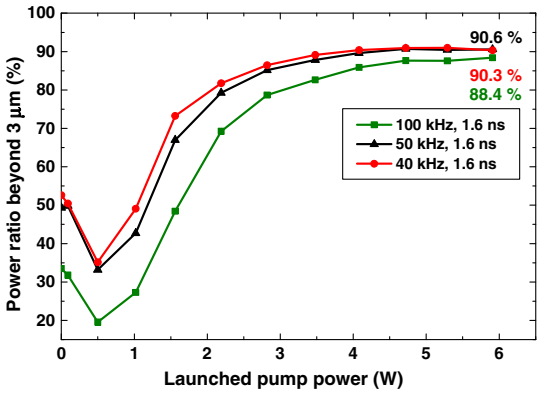

Fig. 5. Power ratio beyond 3 μm under PRR of 40, 50, and 100 kHz.

produced at a slope efficiency of 7.1% (11%) with respect to launched (absorbed) pump power. It should be noted that no cascade lasing at 2.1 μm was observed in spectrum in the full pump power range. Besides, insufficient pump absorption due to a small cladding absorption coefficient (~1 dB/m) and the limited length of HDZF (4.5 m) were mainly responsible for the obvious disparity between the slope efficiency with respect to launched pump power (7.1%) and that with respect to absorbed pump power (11%). Considering the total pump absorption of 4.5 dB, i.e., 64.5%, a large portion of the launched pump light was unabsorbed and wasted. Therefore, a longer piece of HDZF was beneficial to obtain a higher output power.

In order to investigate the power ratio beyond 3 μm, a spectral integral with respect to launched pump power was calculated and was plotted in Fig. 5. Take 50 kHz, 1.6 ns as an example. A power ratio beyond 3 μm first decreased from ~50% to ~35% at the first 0.5 W pump power range, since the spectral intensity increase was mainly focused on the amplification of the 2.9–3.0 μm region, and no obvious frequency shift was observed. Then the power ratio increased sharply to ~80% as launched pump power increased from 0.5 to 2.5 W. For higher pump power of 2.5–4 W, the power ratio was improved slowly to ~90%. Further increasing the pump power made no apparent difference in the power ratio. Under maximum launched pump power of 5.9 W, the power ratio was 90.6% (372 mW in power), which was higher than that of a previously reported MIR-SC erbium-doped fluoride fiber amplifier [17]. This is the highest power portion beyond 3 μm ever achieved in a piece of rare-earth-doped ZBLAN-fiber up to now. Under circumstances of 40 kHz, the power ratio curve has no significant difference compared with that of 50 kHz; a power ratio of 90.3% was obtained under maximum pump power, which was almost identical to that of 50 kHz. Under the circumstance of 100 kHz, the power ratio was basically lower, with a highest value of 88.4%. The characteristics of a power ratio beyond 3 μm fit well with the spectral characteristics in Fig. 3.

3. CONCLUSION

In conclusion, a 411-mW, spectrally flat MIR-SC was directly generated in an HDZFA. Benefiting from the three-stage-cascaded amplification process and frequency-shift process, the obtained SC has an overall spectral range of 2.8–3.9 μm and a 3-dB spectral range of 2.93–3.70 μm. A power ratio beyond 3 μm as high as 90.6% was obtained owing to the use of a $^5I_6 \rightarrow {}^5I_7$ transition of Ho^{3+}, whose emission wavelength is longer than that of the $^4I_{11/2} \rightarrow {}^4I_{13/2}$ transition of Er^{3+}. The obtained SC laser represents a promising pump source for InF_3 or chalcogenide fibers in the purpose of achieving further spectral extension towards the deeper MIR region. To the best of our knowledge, this research demonstrates not only the first in-amplifier spectrally flat MIR-SC generation, but also the highest power ratio beyond 3 μm obtained in rare-earth-doped ZBLAN fiber to date. Once an MIR fiber combiner is available, an all-fiberized configuration of this SC system could be readily obtained, and the compactness, reliability, as well as the slope efficiency of the HDZFA would be improved.

Funding. National Natural Science Foundation of China (NSFC) (61435009).

REFERENCES

1. A. Labruyère, A. Tonello, V. Couderc, G. Huss, and P. Leproux, "Compact supercontinuum sources and their biomedical applications," Opt. Fiber Technol. **18**, 375–378 (2012).
2. G. Méjean, J. Kasparian, E. Salmon, J. Yu, J.-P. Wolf, R. Bourayou, R. Sauerbrey, M. Rodriguez, L. Wöste, and H. Lehmann, "Towards a supercontinuum-based infrared lidar," Appl. Phys. B **77**, 357–359 (2003).
3. H. T. Bekman, J. Van Den Heuvel, F. Van Putten, and R. Schleijpen, "Development of a mid-infrared laser for study of infrared countermeasures techniques," in *European Symposium on Optics and Photonics for Defence and Security* (2004), pp. 27–38.
4. A. Mukherjee, S. Von der Porten, and C. K. N. Patel, "Standoff detection of explosive substances at distances of up to 150 m," Appl. Opt. **49**, 2072–2078 (2010).
5. X. Zou and T. Izumitani, "Spectroscopic properties and mechanisms of excited state absorption and energy transfer upconversion for Er^{3+}-doped glasses," J. Non-Cryst. Solids **162**, 68–80 (1993).
6. K. Yin, R. Zhu, B. Zhang, T. Jiang, S. Chen, and J. Hou, "Ultrahigh-brightness, spectrally-flat, short-wave infrared supercontinuum source for long-range atmosphe-reic applications," Opt. Express **24**, 20010–20020 (2016).
7. G. Qin, X. Yan, C. Kito, M. Liao, C. Chaudhari, T. Suzuki, and Y. Ohishi, "Ultrabroadband supercontinuum generation from ultraviolet to 6.28 μm in a fluoride fiber," Appl. Phys. Lett. **95**, 161103 (2009).
8. J.-C. Gauthier, V. Fortin, J.-Y. Carrée, S. Poulain, M. Poulain, R. Vallée, and M. Bernier, "Mid-IR supercontinuum from 2.4 to 5.4 μm in a low-loss fluoroindate fiber," Opt. Lett. **41**, 1756–1759 (2016).
9. R. Thapa, D. Rhonehouse, D. Nguyen, K. Wiersma, C. Smith, J. Zong, and A. Chavez-Pirson, "Mid-IR supercontinuum generation in ultra-low loss, dispersion-zero shifted tellurite glass fiber with extended coverage beyond 4.5 μm," Proc. SPIE **8898**, 889808 (2013).
10. R. R. Gattass, L. Brandon Shaw, V. Q. Nguyen, P. C. Pureza, I. D. Aggarwal, and J. S. Sanghera, "All-fiber chalcogenide-based mid-infrared supercontinuum source," Opt. Fiber Technol. **18**, 345–348 (2012).
11. X. Zhu and N. Peyghambarian, "High-power ZBLAN glass fiber lasers: review and prospect," Adv. OptoElectron. **2010**, 501956 (2010).
12. L.-R. Robichaud, V. Fortin, J.-C. Gauthier, S. Châtigny, J.-F. Couillard, J.-L. Delarosbil, R. Vallée, and M. Bernier, "Compact 3–8 μm supercontinuum generation in a low-loss As_2Se_3 step-index fiber," Opt. Lett. **41**, 4605–4608 (2016).
13. C. Xia, Z. Xu, M. N. Islam, J. F. L. Terry, M. J. Freeman, A. Zakel, and J. Mauricio, "10.5 W time-averaged power mid-IR supercontinuum generation extending beyond 4 μm with direct pulse pattern modulation," IEEE J. Sel. Top. Quantum Electron. **15**, 422–434 (2009).

14. K. Liu, J. Liu, H. Shi, F. Tan, and P. Wang, "High power mid-infrared supercontinuum generation in a single-mode ZBLAN fiber with up to 21.8 W average output power," Opt. Express **22**, 24384–24391 (2014).
15. K. Yin, B. Zhang, L. Yang, and J. Hou, "15.2 W spectrally flat all-fiber supercontinuum laser source with >1 W power beyond 3.8 μm," Opt. Lett. **42**, 2334–2337 (2017).
16. J. Liu, J. Xu, K. Liu, F. Z. Tan, and P. Wang, "High average power picosecond pulse and supercontinuum generation from a thulium-doped all-fiber amplifier," Opt. Lett. **38**, 4150–4153 (2013).
17. J.-C. Gauthier, V. Fortin, S. Duval, R. Vallée, and M. Bernier, "In-amplifier mid-infrared supercontinuum generation," Opt. Lett. **40**, 5247–5250 (2015).
18. J. Swiderski and M. Michalska, "Mid-infrared supercontinuum generation in a single-mode thulium-doped fiber amplifier," Laser Phys. Lett. **10**, 035105 (2013).
19. V. V. Dvoyrin and I. T. Sorokina, "All-fiber optical supercontinuum sources in 1.7–3.2 μm range," Proc. SPIE **8961**, 89611C (2014).
20. K. Yin, B. Zhang, J. Yao, L. Yang, G. Liu, and J. Hou, "1.9–3.6 μm supercontinuum generation in a very short highly nonlinear germania fiber with a high mid-infrared power ratio," Opt. Lett. **41**, 5067–5070 (2016).
21. J. Schneide, C. Carbonnier, and U. B. Unrau, "Characterization of a Ho^{3+}-doped fluoride fiber laser with a 3.9-μm emission wavelength," Appl. Opt. **36**, 8595–8600 (1997).